Received 16 April 2020; | Revised 6 June 2020; | Accepted 6 June 2020

DOI: xxx/xxxx

ARTICLE TYPE

Quartic Trigonometric Tension B-spline Finite Element Method for Solving Gardner Equation

Ozlem Ersoy Hepson*

[1]Mathematics-Computer Department, Eskisehir Osmangazi University, Eskisehir, Turkey

Correspondence
Email: ozersoy@ogu.edu.tr

Present Address
Mathematics-Computer Department, Science and Letters Faculty, Eskisehir Osmangazi University

Summary

Method of collocation is established for getting solution of the Gardner equation (GE). The GE is fully integrated by way of the Crank-Nicolson method for time variable and collocation method for spatial variable. Trial function of the collocation method is set up using combination of quartic trigonometric tension (QTT) B-splines. Convergence analysis of suggested method is investigated. Performance of the quartic trigonometric tension B-splines is searched by studying three test problems; propagation of bell shape solitary wave, interaction of two positive bell shape solitary wave and wave generation.

KEYWORDS:
quartic trigonometric tension B-spline, Gardner equation, convergence analysis, solitary wave, wave generation

1 | INTRODUCTION

Numerical methods are powerful tools for solving partial differential equations(PDEs). With advent of computer technology, variants of the finite element codes have been developed to solve PDEs irrespective of the shape of the problem domain and types of the boundary conditions(BCs). Accuracy of the finite element formulation is increased by a suitable mesh refinement and selection of the basis functions. The finite element method based on spline functions are applied to so many differential equations and high accuracy have been obtained. In the finite element method, the unknown function of differential equations and its derivatives over each elements is represented as linear combination of both undetermined time parameters and spline functions. The B-splines are popularly applied in solving the differential equations. To beat the limitation of the B-splines especially for constructing curve and surfaces discussed in [1], useful non-polynomial B-splines, such as exponential B-splines, trigonometric B-splines, hyperbolic B-splines and etc. [1] have bee proposed. The trigonometric quartic B-splines is type of non-polynomial splines which are used to construct a finite element code for solving the GE. In this study, the unknown variables are approximated by a linear combination of the trigonometric tension B-spline functions, which are a variant of polynomial B-spline basis functions. Thus finite element method accommodated the QTT B-spline is built up for the GE. Performance of the QTT B-spline finite element method will be evaluated for the GE. Combination of the KDV equation and Modified KDV equation GE which has the following form

$$u_t + \mu_1 u u_x + \mu_2 u^2 u_x + \mu_3 u_{xxx} = 0 \tag{1}$$

in which there exist evolution term u_t,two nonlinear terms uu_x and u^2u_x and third order dissipative term u_{xxx}. The initial condition (IC)

$$u(x,0) = u_0(x) \tag{2}$$

[0]**Abbreviations:** GE, Gardner equation; QTT, Quartic Trigonometric tension; IC, initial condition; BC, Boundary condition; ARC, Absolute relative changes

and the homogen Dirichlet and Neumann conditions at both end of the interval $[a, b]$ for the mathematical representation of the initial boundary value problem. The competition of three spatial derivative terms and their constant constitutes main interest of solution behaviour of GE for scientist. Thus Selection of constants μ_1, μ_2 and μ_3, and terms specifies some significant modes of internal waves with large amplitudes and weakly nonlinear dispersive waves, undular bore in the bright and dark cnoidals, trigonometric bores, kinks[2], negative ion-acoustic plasma waves[3], occurrence of large ocean waves in unexpected meaning and determination of the modulational instability in same cases[4].

Analytical and semi-analytical solutions are restricted for GE. Analytical methods with is special solutions have been given in some papers, for instance transcritical flow of a fluid passing a local topographical obstacle[5], collision of a large amplitude solution with a limiting soliton[6], a large class of interaction solutions of solitons with cnoidal and periodic waves[7], some collusion models of cnoidal wave to soliton[8], some hyperbolic type solitary wave and periodic solutions expressed in the finite series form[9] and a bunch of traveling wave type exact solutions[10].

Numerical methods are also obtained both to affirm analytical behaviors and to provide non-analytical solution of GE with some ICs and BCs. A multi-symplectic method[11] and a multi-symplectic Fourier pseudospectral scheme[12] are developed for the GE respectively. The finite difference and restrictive Taylor's approximation are constructed to determine the numerical solutions to the GE[13,14]. Linear conservative finite volume element schemes is applied for solving the GE. Quintic B-spline differential quadrature method has been used to obtain the numerical approximation of the GE[15]. Collocation method based on quintic, exponential and extended cubic B-splines are set up for solving the GE in the studies[16,17,18]. Solutions of the fractional GE with collocation method using radial basis function is given in the work[19].

There are few numerical method build up using the trigonometric tension spline for solving differential equations. The tension B-spline collocation method is used for finding the solutions of IBVPs in study[20] and the technique is applied for finding solutions of Burgers-Huxley equation[21]. In the present study, the construction of QTT B-spline collocation algorithms to the GE is done. The convergence analysis is discussed. Some test problems including bell shape solitary wave, interaction of two positive bell shape solitary wave and wave generation are studied.

2 | QTT B-SPLINE COLLOCATION METHOD

A nonpolynomial spline possesses smootness depending on the its degree over the interval. The uniform partition of the interval $[a, b]$ is considered by knots $x_i = a + ih$, where $a = x_0, b = x_N$ and $h = (b - a)/N$. The knots and additional fictitious knots $x_{-4}, x_{-3}, x_{-2}, x_1, x_{n+1}, x_{n+1}, x_{n+2}, x_{n+3}$ outside the interval to have a basis of QTT B-spline over the interval the interval is needed. Thus QTT B-splines have the following form:

$$T_{i,5}(x) = r\begin{cases} \frac{\tau^2(-D_{i-2})^2+2C_{i-2}-2}{2\tau^2}, & \left[x_{i-2}, x_{i-1}\right], \\ -\frac{\tau^2(3h^2+6hD_{i-2}+2(-D_{i-2})^2)+2M_1(\tau^2(D_{i-1})^2-2)-(6C_{i-1}+2C_i-4)}{2\tau^2}, & \left[x_{i-1}, x_i\right], \\ \frac{\tau^2\left(13h^2+10hD_{i-2}+2(-D_{i-2})^2\right)+M_1(2\tau^2(11h^2+10hD(i-2))+4M_1\tau^2(-D_{i-2})^2-8M_1+6C_{i+1}-4)}{2\tau^2}, & \left[x_i, x_{i+1}\right], \\ -\frac{\tau^2(23h^2+14h(D_{i-2})+2(-D_{i-2})^2)+2M_1(\tau^2(D_{i+2})^2-2)-(2C_{i+1}+6C_{i+2}-4)}{2\tau^2}, & \left[x_{i+1}, x_{i+2}\right], \\ \frac{\tau^2(D_{i+3})^2+2C_{i+3}-2}{2\tau^2}, & \left[x_{i+2}, x_{i+3}\right], \\ 0, & \text{otherwise.} \end{cases} \tag{3}$$

where $r = \frac{1}{2h^2(1-M_1)}$, $C_{i+j} = \cos(\tau(x_{i+j} - x))$, $D_{i+j} = (x_{i+j} - x)$, $M_1 = \cos(\tau h)$, $M_2 = \sin(\tau h)$, which was suggested as a variant of UE splines in the work[22] in which UE-spline basis functions of order $k = 2$ and derivation of high order UE-splines, when degree $k \geq 2$, are introduced. It is a piecewise non-polynomial bell-shape function whose values at the connecting point can be calculated as Table 1.

The shape of QTT B-spline can be changed by varying the free parameter τ and when $\tau = 5$, graph of the QTT B-spline is depicted in Figure 1.

TABLE 1 $T_i(x)$ and its derivatives

	x_{i-2}	x_{i-1}	x_i	x_{i+1}	x_{i+2}	x_{i+3}
$T_{i,5}$	0	$r\left(\frac{h^2\tau^2+2M_1-2}{2\tau^2}\right)$	$r\left(\frac{h^2\tau^2-2M_1\left(h^2\tau^2+1\right)+2}{2\tau^2}\right)$	$r\left(\frac{h^2\tau^2-2M_1\left(h^2\tau^2+1\right)+2}{2\tau^2}\right)$	$r\left(\frac{h^2\tau^2+2M_1-2}{2\tau^2}\right)$	0
$T'_{i,5}$	0	$r\left(\frac{h\tau-M_2}{\tau}\right)$	$-r\left(\frac{h\tau-3M_2+2M_1h\tau}{\tau}\right)$	$r\left(\frac{h\tau-3M_2+2M_1h\tau}{\tau}\right)$	$-r\left(\frac{h\tau-M_2}{\tau}\right)$	0
$T''_{i,5}$	0	$r(1-M_1)$	$r(-1+M_1)$	$r(-1+M_1)$	$r(1-M_1)$	0
$T'''_{i,5}$	0	$r(\tau M_2)$	$-r(3\tau M_2)$	$r(3\tau M_2)$	$-r(\tau M_2)$	0

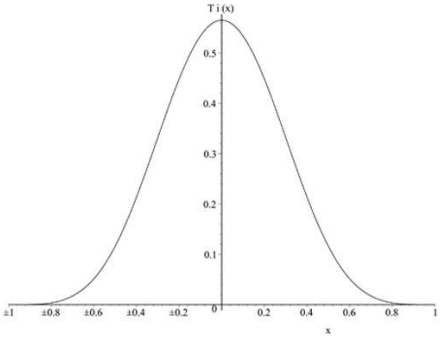

FIGURE 1 QTT B-splines over the interval $[-1, 1]$ for $\tau = 5$

Since $T_{i,5}(x)$ are the basis function for space $\left\{\cos(\tau x), \sin(\tau x), x^{k-3}, \ldots, x, 1\right\}$ of the trigonometric and polynomial functions, approximate the unknown function u and its derivatives u_t, u_{xx}, u_{xxx} with and its derivatives U_t, U_x, U_{xxx} respectively consisting of combination of QTT B-splines as

$$U(x,t) = \sum_{i=-2}^{N+1} c_i(t) T_i(x) \tag{4}$$

where $c_i(t)$ represent time-dependent quantities which will be calculated by using collocation method.

U and its first three derivatives at the connecting points can be computed using QTT B-splines[21] and approximation (4)

$$\begin{aligned} u(x_i,t_n) &\approx U_i^n = v_1c_{i+1} + v_2c_i + v_2c_{i-1} + v_1c_{i-2}, \\ u_x(x_i,t_n) &\approx (U')_i^n = z_1c_{i+1} + z_2c_i - z_2c_{i-1} - z_1c_{i-2}, \\ u_{xx}(x_i,t_n) &\approx (U'')_i^n = w_1c_{i+1} + w_2c_i + w_2c_{i-1} + w_1c_{i-2} \\ u_{xxx}(x_i,t_n) &\approx (U''')_i^n = y_1c_{i+1} + y_2c_i + y_2c_{i-1} + y_1c_{i-2} \end{aligned} \tag{5}$$

with

$$\begin{aligned} v_1 &= r\left(\frac{h^2\tau^2+2M_1-2}{2\tau^2}\right),\ v_2 = r\left(\frac{h^2\tau^2-2M_1\left(h^2\tau^2+1\right)+2}{2\tau^2}\right) \\ z_1 &= r\left(\frac{h\tau-M_2}{\tau}\right),\ z_2 = -r\left(\frac{h\tau-3M_2+2M_1h\tau}{\tau}\right) \\ w_1 &= r(1-M_1),\ w_1 = r(-1+M_1), \\ y_1 &= r(\tau M_2),\ y_2 = -r(3\tau M_2), \\ M_1 &= \cos(\tau h),\ M_2 = \sin(\tau h) \end{aligned}$$

Time integration of the GE (1) can be managed by employing using Crank-Nicolson method, and obtain semi-integrated the GE of the form:

$$\frac{U^{n+1}-U^n}{\Delta t}+\mu_1\frac{(UU_x)^{n+1}+(UU_x)^n}{2}+\mu_2\frac{(U^2U_x)^{n+1}+(U^2U_x)^n}{2}+\mu_3\frac{U^{n+1}_{xxx}+U^n_{xxx}}{2}=0 \tag{6}$$

where $t^n=t^{n-1}+\Delta t$ and Δt is the time step, for approximate solution $U^n=U(x,t^n)$ at the nth time level.

Before applying the collocation method, linearization

$$(UU_x)^{n+1}=U^nU_x^{n+1}+U_x^nU^{n+1}-U^nU_x^n$$

and

$$(U^2U_x)^{n+1}=2U^nU_x^nU^{n+1}+(U^n)^2U_x^{n+1}-2U_x^n(U^n)^2$$

which are obtained from the Taylor expansion, is applied to Eq. (6) to obtain

$$\begin{aligned}&\left(1+\mu_1\frac{\Delta t}{2}U_x^n+\mu_1\Delta tU^nU_x^n\right)U^{n+1}+\frac{\Delta t}{2}\left(\mu_1U^n+\mu_2(U^n)^2\right)U_x^{n+1}+\mu_3\frac{\Delta t}{2}U^{n+1}_{xxx}\\&=U^n+\mu_2\frac{\Delta t}{2}(U^n)^2U_x^n-\mu_3\frac{\Delta t}{2}U^n_{xxx}\end{aligned} \tag{7}$$

By substituting approximations in(5) into (7),the fully-integrated equation with the unknown coefficients c_i, $i=-2,\cdots,N+1$, is obtained

$$a_1c^{n+1}_{i-2}+a_2c^{n+1}_{i-1}+a_3c^{n+1}_i+a_4c^{n+1}_{i+1}=\mathbf{B}^n_i,\ i=0,1,\cdots,N \tag{8}$$

where

$$\mathbf{B}^n_i=U^n_i+\mu_2\frac{\Delta t}{2}(U^n_i)^2\left(U'\right)^n_i-\mu_3\frac{\Delta t}{2}\left(U'''\right)^n_i,\ i=-2,-1,\cdots,N+1 \tag{9}$$

and

$$\begin{aligned}a_1&=b_1v_1-b_2z_1+b_3y_1,\ a_2=b_1v_2-b_2z_2+b_3y_2\\a_3&=b_1v_2+b_2z_2+b_3y_2,\ a_4=b_1v_1+b_2z_1+b_3y_1\end{aligned} \tag{10}$$

with

$$\begin{aligned}b_1&=1+\mu_1\frac{\Delta t}{2}U_x^n+\mu_1\Delta tU^nU_x^n,\\b_2&=\frac{\Delta t}{2}\left(\mu_1U^n+\mu_2(U^n)^2\right),\\b_3&=\mu_3\frac{\Delta t}{2}.\end{aligned}$$

Finally, $(N+1)$ linear algebraic equations in $(N+4)$ unknown are derived. Elimination of unknown parameters c^{n+1}_{-2}, $c^{n+1}_{-1}$and c^{n+1}_{n+4} using the BCs $u(a,t)=u_x(a,t)=0$ and $u(b,t)=0$, to get additional three equations

$$\begin{aligned}&u(a,t_n)\approx U^n_0=v_1c^n_1+v_2c^n_0+v_2c^n_{-1}+v_1c^n_{-2}=0,\\&u_x(a,t_n)\approx(U')^n_0=-z_1c_1-z_2c_0+z_2c_{-1}+z_1c_{-2}=0,\\&u(b,t_n)\approx U^n_0=v_1c_1+v_2c_0+v_2c_{-1}+v_1c_{-2}=0,\end{aligned} \tag{11}$$

leads to $(N+1)\times(N+1)$ solvable system as

$$\mathbf{Ax}=\mathbf{B} \tag{12}$$

where

$$\mathbf{A}=\begin{bmatrix}v_1&v_2&v_2&v_1&&&&\\-z_1&-z_2&z_2&z_1&&&&\\&a_1&a_2&a_3&a_4&&&\\&&\ddots&\ddots&\ddots&\ddots&&\\&&&a_1&a_2&a_3&a_4&\\&&&&v_1&v_2&v_2&v_1\end{bmatrix}$$

$$\mathbf{x}=\left(c^{n+1}_{-2},c^{n+1}_{-1},\cdots,c^{n+1}_{N+1}\right)$$

and

$$\mathbf{B}=\left(0,0,\mathbf{b}^n_{-2},\mathbf{b}^n_{-1},\cdots,\mathbf{b}^n_{N+1},0\right)^T.$$

3 | CONVERGENCE ANALYSIS

Lemma: If $\{T_{-2}, T_{-1}, \cdots, T_{N+1}, \}$ is QTT B-Splines, then

$$\sum_{i=-2}^{N+1} |T_i(x)| \leq \frac{35}{24}, \ a \leq x \leq b. \tag{13}$$

Proof See reference[21].

Theorem: If $Y(x) \in C^5[a, b]$, then constants k_i, exists independent of h in such a way that

$$\left\| D^i y - D^i Y \right\|_\infty \leq k_i h^{5-i}, \ i = 0, 1, 2, 3. \tag{14}$$

Proof See reference[23].

Theorem: If $u(x,t)$ be the exact solution of (2) and $u(x,t) \in C^5[a,b]$ also $\left|\frac{\partial^5 u(x,t)}{\partial x^5}\right| \leq L$ and $U(x,t)$ be the numerical approximation by present method, then

$$\|U(x,t) - u(x,t)\|_\infty \leq O(h^3 + \Delta t). \tag{15}$$

Proof At the $(n+1)th$ time step, let S^* be the unique spline interpolate to the exact solution u of (1)-(2) as follows

$$S^*(x) = \sum_{i=-2}^{N+1} c^* T_i(x) \tag{16}$$

Matrix $\mathbf{A}$ is regarded as a strictly diagonally dominant matrix. Let η_i $(1 \leq i \leq N+1$ be the summation of the ith row of the matrix $\mathbf{A}$. Let a_{ki}^{-1} be the elements of $\mathbf{A}^{-1}$, then following equation can be written using theory of matrices:

$$\sum_{i=1}^{N+1} a_{ki}^{-1} \eta_i = 1. \tag{17}$$

Therefore, it can be find that

$$\left\|\mathbf{A}^{-1}\right\|_\infty = \sum_{i=1}^{N+1} \left|a_{ki}^{-1}\right| \leq \frac{1}{\min_{1 \leq i \leq N+1} \eta_i} \leq \frac{1}{K} \tag{18}$$

where K is constant. By changing $S^*(x)$ in (6), it can be obtained

$$\mathbf{A}\mathbf{x}^* = \mathbf{B}^*. \tag{19}$$

Subtracting (12), (19) and infinity norm is applied, the following equation is provided

$$\|\mathbf{x}^* - \mathbf{x}\|_\infty \leq \left\|\mathbf{A}^{-1}\right\|_\infty \|\mathbf{B}^* - \mathbf{B}\|_\infty . \tag{20}$$

By applying (8) and (14), it can be written

$$\begin{aligned} \left|\mathbf{b}_i^* - \mathbf{b}_i\right| &\leq \left|b_1 \left(S^*(x_i) - U(x_i)\right)\right| + \left|b_2 \left(S^{*\prime}(x_i) - U'(x_i)\right)\right| + \left|b_3 \left(S^{*\prime\prime}(x_i) - U''(x_i)\right)\right| \\ &\leq \left|b_1\right| k_0 h^5 + \left|b_2\right| k_1 h^4 + \left|b_3\right| k_2 h^3. \end{aligned} \tag{21}$$

From (21), it can be derived

$$\|\mathbf{B}^* - \mathbf{B}\|_\infty \leq K_1 h^3, \tag{22}$$

where $K_1 = \left|b_1\right| k_0 h^2 + \left|b_2\right| k_1 h + \left|b_3\right| k_2$. Therefore, by appliying norm and from Lemma 1, (18), (20) and (22), it can be written

$$\|\mathbf{S}^*(x) - U(x)\|_\infty = \left\| \sum_{i=-2}^{N+2} \left(c_i^* - c_i\right) T_i(x) \right\|_\infty \leq \left| \sum_{i=-2}^{N+2} T_i(x) \right| \|\mathbf{x}^* - \mathbf{x}\|_\infty \leq \frac{35}{24} K_2 h^2 \tag{23}$$

where $K_2 = \frac{K_1}{G}$ is constant. From Theorem 1, it can be obtained

$$|u(x) - S^*(x)| \leq k_0 h^5 \tag{24}$$

and by using (23) and (24), it can be concluded that

$$\|U(x) - u(x)\|_\infty \leq \|\mathbf{S}^*(x) - U(x)\|_\infty + \|u(x) - \mathbf{S}^*(x)\|_\infty \leq \frac{35}{24} K_2 h^3 + k_0 h^5 = \gamma h^3 \tag{25}$$

where $\gamma = \frac{35}{24} K_2 + k_0 h^2$.

4 | NUMERICAL EXAMPLES

Three test problems will be studied to see performance of the suggested algorithm and finding results are compared with those obtained with the quintic B-spline collocation method [16] in terms of discrete maximum error norm:

$$L_\infty(t) = |U(x,t) - u(x,t)|_\infty = \max_i \left|U(x_i,t) - u(x_i,t)\right|$$

GE is shown to keep the lowest three conservation laws, the momentum (M), the energy (E) and the Hamiltonian (H) described by

$$\begin{aligned} M &= \int_{-\infty}^{\infty} u dx \approx \int_a^b u dx \approx h\sum_{j=1}^{N} u_j \\ E &= \int_{-\infty}^{\infty} u^2 dx \approx \int_a^b u^2 dx \approx h\sum_{j=1}^{N} u_j^2 \\ H &= \int_{-\infty}^{\infty} \left(\frac{\mu_1 u^3}{3} + \frac{\mu_2 u^4}{6} - \mu_3 (u_x)^2\right) dx \\ &\approx \int_a^b \left(\frac{\mu_1 u^3}{3} + \frac{\mu_2 u^4}{6} - \mu_3 (u_x)^2\right) dx \\ &\approx h\sum_{j=1}^{N} \left(\frac{\mu_1 u_j^3}{3} + \frac{\mu_2 u_j^4}{6} - \mu_3 (u_x)_j^2\right) \end{aligned} \tag{26}$$

Absolute relative changes (ARCs), $C(M_t)$, $C(E_t)$ and $C(H_t)$

$$\begin{aligned} C(M_t) &= \left|\frac{M_t - M_0}{M_0}\right| \\ C(E_t) &= \left|\frac{E_t - E_0}{E_0}\right| \\ C(H_t) &= \left|\frac{H_t - H_0}{H_0}\right| \end{aligned} \tag{27}$$

are computed to give conservation laws at time t, where subscripts 0 denotes conserved constant at $t = 0$.

4.1 | Propagation of Bell Shape Solitary Wave

To be able to make comparison between numerical and analytical solutions, solitary wave solution of GE is studied to see advance of wave during running time of the algorithm, which is defined analytically in some studies [16,24] as

$$\begin{aligned} u(x,t) &= S\sec h(k(x - x_0 - ct)) \\ k = \sqrt{\frac{c}{\mu_3}} \text{and } S &= \frac{6c}{\mu_1(1 + \sqrt{1 + 6\frac{\mu_2 c}{\mu_1^2}})} \end{aligned} \tag{28}$$

With parameters $\mu_1 = 1$, $\mu_2 = 1$, $\mu_3 = 5$ and $x_0 = 0$, initial profiles, having bell-type shape is locate along the x-axis centered at $x = 0$ in the restricted region $[-100, 100]$. Three BCs are used to have solvable system of algebraic equations: two of them are on left, $u(-100,t)$ and $u_x(-100,t)$ and one is on the right, $u(100,t) = 0$ to have solvable with system of equation. The program is run up to time $t = 5$ with time increment $\Delta t = 0.01$ and space increment $h = 0.1$. The propagation of the waves is managed without deforming the shape seen in the Figure 2 (a). Error distribution along problem domain is exhibited in Figure 2(b) in which errors at some times can be observed and error variation remain almost constant, changes from 0.000175 at time $t = 1$ to 0.000911 at time $t = 5$ happens within difference 0.000736. Discrete maximum error norms at times $t = 1, 2, 3, 4, 5$ and ARCs are documented in Table 2. Almost constant relative changes endorse lower increase of error during run of the algorithm. In the

same table, numerical solution of the GE using quintic collocation methods is added to make comparison, from which suggested method provide similar results with the quintic collocation method. Thus lower cost algorithm is our achievement for paper. Approximate M, E and H at $t = 0$ is calculated as $M_0 = 3.497319$, $E_0 = 0.192200$ and $H_0 = 0.002578$. Relative changes $C(E_5)$ vary far less then $C(M_5)$ and $C(H_5)$.

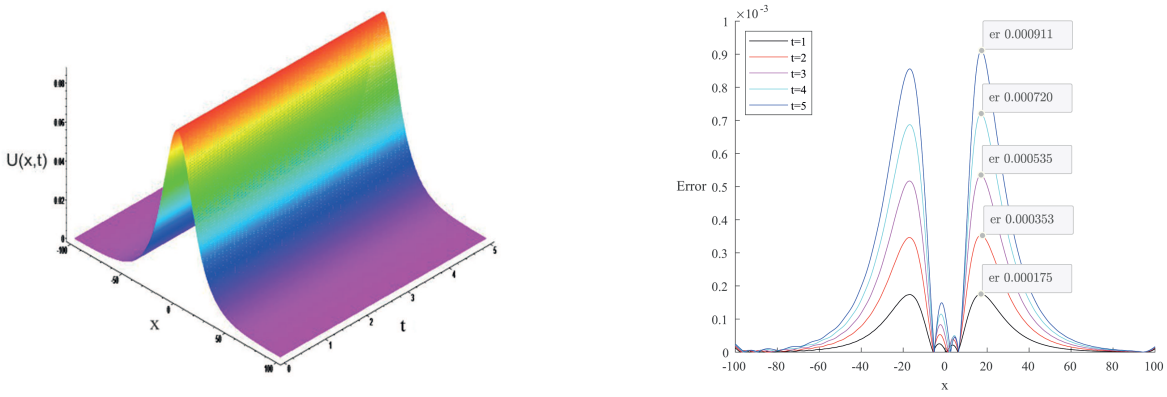

(a) The numerical solution in 3D

(b) The maximum error distribution

FIGURE 2 Propagation of the bell shape solitary and the discrete maximum error distributions at $\Delta t = 0.01$ with $h = 0.1$

TABLE 2 The discrete maximum error norms and the ARCs for the propagation of the bell shape solitary wave

t	L_∞ Suggested Method	Collocation method[16]	$C(M_5)$	$C(E_5)$	$C(H_5)$
1	1.757302^{-4}	2.537778×10^{-4}	5.8992×10^{-6}	1.76×10^{-8}	4.604×10^{-7}
2	3.538030^{-4}	4.182652×10^{-4}	9.6121×10^{-6}	2.93×10^{-8}	1.2881×10^{-6}
3	5.352958^{-4}	6.099896×10^{-4}	1.28291×10^{-5}	3.98×10^{-8}	2.6151×10^{-6}
4	7.209791^{-4}	7.817635×10^{-4}	1.56944×10^{-5}	4.92×10^{-8}	4.4206×10^{-6}
5	9.116738^{-4}	9.583943×10^{-4}	1.84480×10^{-5}	5.84×10^{-8}	6.7084×10^{-6}

4.2 | Interaction of two Positive Bell Shape Solitaries

The interaction of two positive bell shape solitaries are also studied using IC[16]:

$$u(x,0) = S_1 sech(k_1(x - x_1)) + S_2 sech(k_2(x - x_2)) \tag{29}$$

$$k_i = \sqrt{\frac{c_i}{\mu_3}},\ S_i = \frac{6c_i}{\mu_1(1 + \sqrt{1 + 6\frac{\mu_2 c_i}{\mu_1^2}})},\ i = 1, 2.$$

This initial condition gives two positive bell shaped solitaries of heights0.26492 and 0.67377 positioned at $x = -25$ and $x = 25$, respectively, at the beginning, Figure 3 (b). Both solitaries propagate to the left along the x -axis as time goes. The parameters are selected as $\mu_1 = 1$, $\mu_2 = 1$ and $\mu_3 = 5$ in the GE. The program is run up to the terminating time $t = 400$ with $h = 0.5$ and $\Delta t = 0.25$ in the finite problem interval $[-750, 150]$ in Fig. 3 (a).

When the time reaches $t = 100$, it is observed that the interaction has started, Fig. 3 (c). The height of the higher solitary is measured as 0.60134 and its peak is located as $x = -0.5$. The height of the lower is determined to be 0.24362 at vertex position.

The height of the higher wave reaches 0.38327 as the height of the lower one 0.39385 at the time $t = 200$, in Fig. 3 (d). The peaks of both the higher and the lower solitaries are located at $x = -25$ and $x = -38.5$, respectively. When the time reaches $t = 300$, the solitaries begin to separate seen in Fig. 3 (e). The height of the higher one increases to 0.58285 and it is located at $x = -64.5$. The peak of the lower one is positioned at $x = -33$ and the height of it decreased to 0.23526. At the end of the simulation, it can be observed that both solitaries are separated and return to their original shapes and heights, Fig. 3 (f). The heights of both solitaries are determined as 0.60839 and 0.23355 as the peaks reach $x = -91$ and $x = -40$ as keeping to propagate on their own ways.

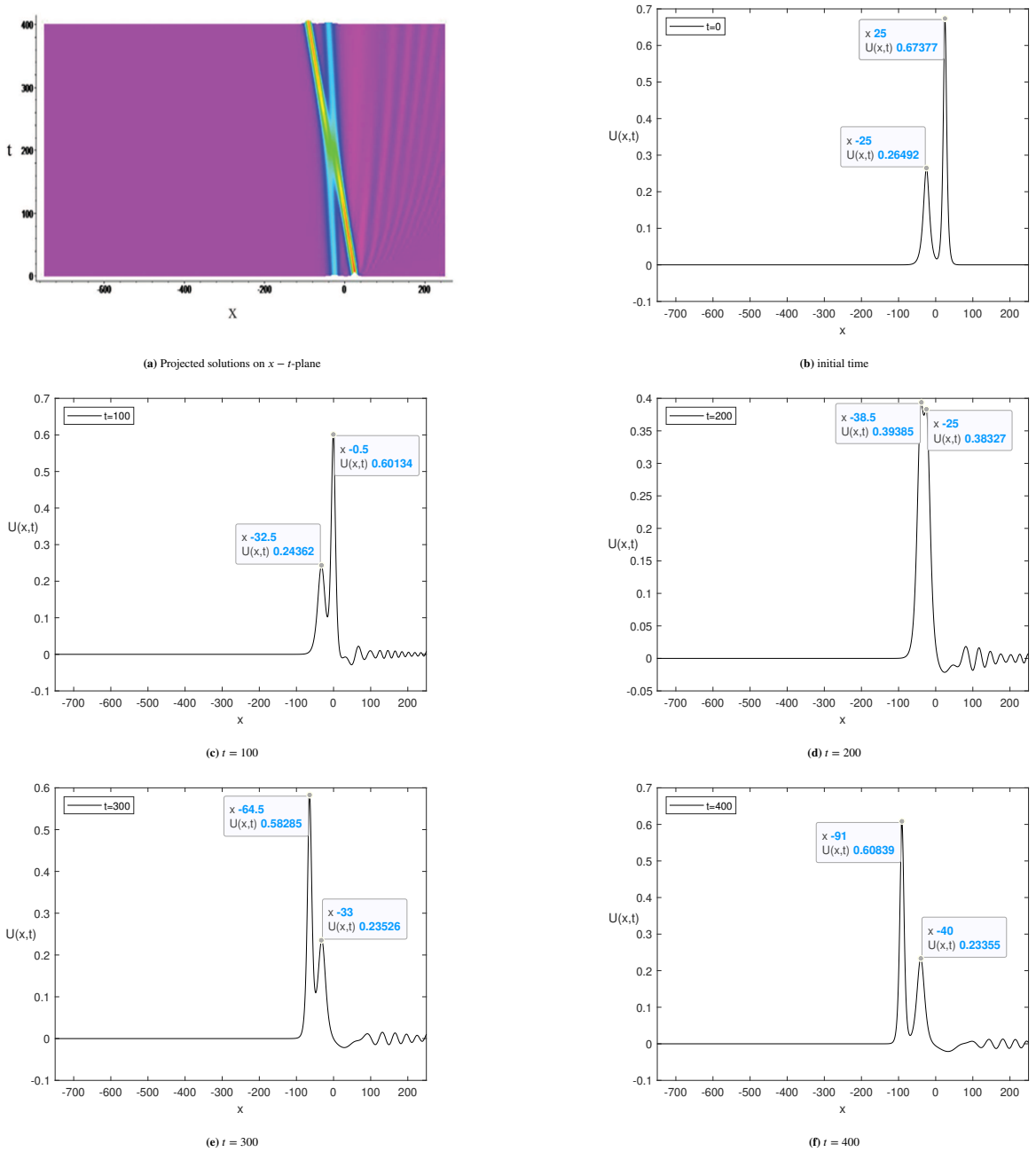

(a) Projected solutions on $x - t$-plane

(b) initial time

(c) $t = 100$

(d) $t = 200$

(e) $t = 300$

(f) $t = 400$

FIGURE 3 Interaction of two positive bell shape solitaries

The conservation laws for the interaction of two positive bell shape solitaries are also computed during the simulations. The values are computed as $M_0 = 14.520509$, $E_0 = 4.706662$ and $H_0 = 0.516125$ initially. The conservation laws in terms of ARC are documented in Table 3.

TABLE 3 The ARCs for the interaction of two positive bell shape solitaries

t	$C(M_t)$	$C(E_t)$	$C(H_t)$
0	–	–	–
100	4.4466×10^{-5}	2.9766×10^{-4}	3.7267×10^{-2}
200	2.5543×10^{-4}	9.9528×10^{-4}	9.2225×10^{-2}
300	4.3875×10^{-4}	1.2589×10^{-3}	5.1698×10^{-2}
400	7.2637×10^{-4}	1.7570×10^{-3}	3.9055×10^{-2}

4.3 | Wave generation

For the last test method, the Maxwellian IC

$$u(x, 0) = e^{-x^2} \tag{30}$$

is used to see generation of waves from initial wave profile. Running of the algorithm with increments $h = 0.01$ and $\Delta t = 0.01$ is carried out up to time $t = 12.5$ over interval $[-15, 15]$ and solution behaviors are depicted in graphs of Figs. 4 (a)-(d). Effect of the parameters $\mu_3 = 0.02, 0.01, 0.005$, $\mu_1 = \mu_2 = 1$ is illustrated in Fig 3. Evolution of initial profile is demonstrated into more sequent waves. More wave generation is produced with smaller μ_3. Their amplitudes are given in graphs at time $t = 12.5$ from which leading wave amplitude and subsequent ones are larger, when μ_3 is smaller. The conserved constants M_0, E_0 and H_0 are calculated as 1.772453, 1.253314 and 0.463747. The conservation laws in terms of ARCs are tabularised in Table 4.

TABLE 4 The ARCs for the wave generation for $\mu_3 = 0.02$

t	$C(M_t)$	$C(E_t)$	$C(H_t)$
2.5	9.7331×10^{-9}	1.4812×10^{-4}	4.8205×10^{-3}
5	2.3957×10^{-8}	1.0136×10^{-4}	6.5932×10^{-4}
7.5	2.5177×10^{-7}	4.9941×10^{-5}	7.9778×10^{-4}
10	6.9634×10^{-7}	1.7519×10^{-6}	9.2994×10^{-4}
12.5	9.4468×10^{-7}	5.3053×10^{-5}	1.0616×10^{-3}

5 | CONCLUSIONS

An alternative hybrid Crank-Nicolson-collocation method is constructed for getting numerical solution of the GE. A numerical method using combination of the QTB B-spline in the method of collocation is presented. Achievement of the algorithm is shown to run the program for exhibiting the progress of the propagation of bell shape solitary wave, interaction of two positive bell shape solitary waves and wave generation. The first test problem is studied because analytical solution of wave propagation exist for GE and L_∞-error norm is computed to see maximum difference between analytical and numerical solutions with lower

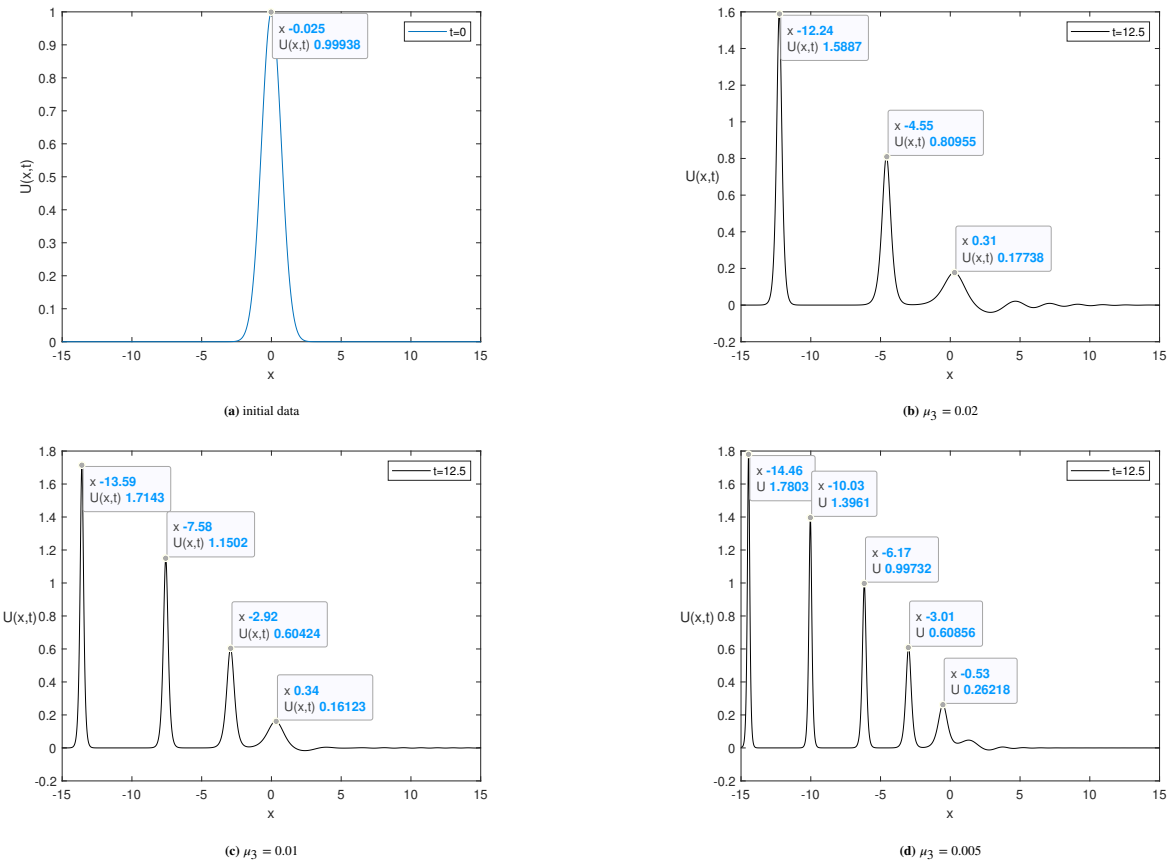

(a) initial data

(b) $\mu_3 = 0.02$

(c) $\mu_3 = 0.01$

(d) $\mu_3 = 0.005$

FIGURE 4 Evolution of wave generation with Maxwellian IC for different values of μ_3

cost. Thus similar results obtained by present Crank-Nicolson-collocation method are provided with quintic collocation method provided in the study [16]. Simulation of interaction and wave generation is observed to see the conservations constants due to not changing their forms. Very slight changes are recorded for amplitudes of both higher and smaller waves as 0.06538 and 0.03137 respectively, after interaction. Thus solitary waves are tried to be kept their shapes even for suggested numerical technique. The relative variation for propagation is much smaller that those variation of the solitary wave interaction as expected. Result of the test problems indicates the reliability of the method to get solutions of the GE. QTT B-spline collocation approach has convergence order 3 in space and order 1 in time. So that nonpolynomial splines provides smooth solutions during run of the program.

References

1. E Mainar, Pena JM, Sanchez-Rayez J. Shape preserving alternatives to the rational Bezier model. *Comput. Aided Geom. Design.* 2001;16:883-906.

2. Kamchatnov AM, Huo YH, Lin TC, et al. Undular bore theory for the Gardner equation. *Physical Review E.* 2012;86(3):036605.

3. Ruderman MS, Talipova T, Pelinovsky E. Dynamics of modulationally unstable ion-acoustic wavepackets in plasmas with negative ions. *J of Plasma Physics.* 2008;74(5):639–565.

4. Grimshaw R, Pelinovsky E, Taipova T, Sergeeva A. Rogue internal waves in the ocean: long wave model. *The European Physical Journal Special Topics.* 2010;185(1):195-208.

5. Kamchatnov AM, Kup YH, Lin TC, et al. Transcritical flow of a stratified fluid over topography: analysis of the forced Gardner equation. *J of Fluid Mechanics.* 2013;736:495-531.

6. Slyunyaev AV, Pelinovsky EN. Dynamics of large-amplitude solitons. *J of Experimental and Theoretical Physics.* 1999;89(1):173-181.

7. Hu H, Tan M, Hu X. New interaction solutions to the combined KdV-mKdV equation from CTE method. *J of the Association of Arab Universities for Basic and Applied Science.* 2016;21:64-67.

8. Wei-Feng Y, Sen-Yue L, Jun Y, Han-wei H. Interactions between Solitons and Cnoidal Periodic Waves of the Gardner Equation. *Chinese Physics Letters.* 2014;31(7):070203.

9. Fu Z, Liu S, Liu S. New kinds of solutions to Gardner equation. *Chaos, Solitons and Fractals.* 2004;20(2):301-309.

10. Wazwaz AM. New solitons and kink solutions for the Gardner equation. *Communications in nonlinear science and numerical simulation.* 2007;12(8):1395-1404.

11. Hu WP, Deng ZC, Qin YY, Zhang RW. Multi-symplectic method for the generalized (2+1)-dimensional KdV-mKdV equation. *Acta Mech Sin.* 2012;28:793-800.

12. Wei Y, Zhang X, Shao Z, Gao JQ, Yang XF. Multi-symplectic integrator of the generalized KdV-type equation based on the variational principle. *Scientific Reports.* 2019;9:15883.

13. Nishiyama H, Noi T. Conservative difference schemes for the numerical solution of the Gardner equation. *Computational and Applied Mathematics.* 2016;35(1):75-95.

14. Rageh TM, Salem G, El-Salam FA. Restrictive Taylor Approximation for Gardner and KdV Equations. *Int. J. Adv. Appl. Math. and Mech.* 2014;1(3):1-10.

15. Yagmurlu NM, Ucar Y, Bashan A. Numerical Approximation of the Combined KdV-mKdV Equation via the Quintic B-Spline Differential Quadrature Method. *Adiyaman University Journal of Science.* 2019;9(2):386-403.

16. Ak T. Numerical experiments for long nonlinear internal waves via Gardner equation with dual-power law nonlinearity. *International Journal of Modern Physics C.* 2019;30(9):1950066.

17. Hepson OE, Korkmaz A, Dag I. Numerical solutions of the Gardner equation by extended form of the cubic B-splines. *Pramana - J Physics.* 2018;91(59):1-10.

18. Hepson OE, Korkmaz A, Dag I. Exponential B-spline collocation solutions to the Gardner equation. *International J of Computer Mathematics.* 2020;97(4):837-850.

19. Kaya D, Gulbahar S, Yokus A, Gulbahar M. Solutions of the fractional combined KdV–mKdV equation with collocation method using radial basis function and their geometrical obstructions. *Advances in Difference Equations.* 2018;2018:77.

20. Alinia N, Zarebnia M. Trigonometric Tension B-Spline Method for the Solution of Problems in Calculus of Variations. *Computational Mathematics and Mathematical Physics.* 2018;58(5):631-641.

21. Alinia N, Zarebnia M. A numerical algorithm based on a new kind of tension B-spline function for solving Burgers-Huxley equation. *Numerical Algorithms.* 2019;82:1121–1142.

22. Wang G, Fang M. Unified and extended form of three types of splines. *J of Computational and Applied Mathematics.* 2008;216:498-508.

23. Jianzhong W, Daren H. On quartic and quintic interpolation splines and their optimal error bounds. *Science in China Series A-Mathematics, Physics, Astronomy and Technological Science.* 1982;25(11):1130-1141.

24. Hamdi S, Morse B, Halphen B, Schiesser W. Conservation laws and invariants of motion for nonlinear internal waves: part II. *Natural hazards.* 2011;57(3):609-616.

AUTHOR BIOGRAPHY

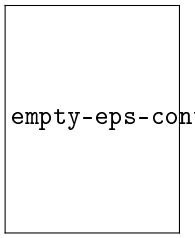

Ozlem Ersoy Hepson. is teaching assistant at the Mathematics-Computer Department, Science and Letters Faculty, Eskişehir Osmangazi University, in Turkey. Dr. Ersoy Hepson received her B.Sc. in 2009 and M.Sc in 2012 from the Eskişehir Osmangazi University. In 2015, she earned Ph.D. in Applied Mathematics from Mathematics-Computer Department, Eskişehir Osmangazi University. Her research interest includes the numerical solutions of the partial differential equations(PDEs) and systems using both spline ïňĄnite element methods and differential quadrature methods. Besides numerical solutions, she also works for exact solutions of PDEs via Ansatz method, Kudryashov method and Sine-Gordon expansion method.

How to cite this article: Williams K., B. Hoskins, R. Lee, G. Masato, and T. Woollings (2016), A regime analysis of Atlantic winter jet variability applied to evaluate HadGEM3-GC2, *Q.J.R. Meteorol. Soc.*, *2017;00:1–6*.